Exploring the Potential of the MandEye Handheld LiDAR System for Mediterranean Understorey Characterisation

Cosme Hernanz-Gilbert [1,3], Carlos Cabo [2], Álvaro Moreno-Martínez [3], and Mónica Herrero-Huerta [1]

[1] Desertification Research Centre (CIDE - CSIC - UV - GVA), Moncada, Valencia, Spain
[2] Department of Mining Exploitation, University of Oviedo, 33004, Oviedo, Spain
[3] Image Processing Laboratory (IPL), Universitat de Valencia, Paterna, València, Spain

Keywords: LiDAR, handheld systems, point cloud processing, understorey, Mandeye, trajectory optimisation.

Abstract

Despite the rapid expansion of Mobile Laser Scanning in forestry, the optimal deployment of affordable handheld LiDAR systems for forest characterisation, particularly at understorey level, remains underexplored. The structural complexity of Mediterranean ecosystems requires highly detailed spatial data to estimate fuel loads, biomass and ecological functioning. This study addresses this gap through an experimental comparison of the open-source MandEye LiDAR device against a premium commercial system, the FARO Orbis Premium, functioning as the ground truth baseline. The research evaluates how pedestrian scanning trajectories, including single loops, multiple concentric loops and complex patterns, affect point cloud quality, understorey volume estimation and structural accuracy within a 10×10 m Mediterranean pine forest plot. Data processing involved point cloud normalisation, tree stem excision to obtain the understorey layer and volumetric modelling via voxelisation and alpha–hull algorithms. Results indicate that trajectory geometry fundamentally dictates SLAM algorithm performance and data reliability. A double concentric loop proved optimal for both devices, overcoming structural occlusion while minimising redundant noise. Conversely, complex trajectories severely penalised SLAM stability, inducing positional drift and structural duplication that wrongly modified and inflated volume metrics. Although the sensor in MandEye exhibited lower canopy penetration compared to FARO, which resulted in a systematic underestimation of internal understorey volume (e.g., 3,31 m^3 bias underestimation during optimal double-loop voxelisation), it successfully captured highly dense and continuous external canopy representations when operated along predictable paths. Ultimately, this study establishes critical methodological guidelines for deploying accessible mobile scanners in forestry.

1. Introduction

Mediterranean ecosystems, which combine riparian with mountainous regions, are shaped by strong spatial heterogeneity, where the understorey layer plays a key role in ecological functioning and management-related questions (Estornell, 2011), such as providing habitat for diverse species, protection against erosion, or its influence on extreme events like fire propagation (Casals, 2016). Unmanned Aerial Vehicles (UAV) are used to mount LiDAR devices and cover large areas of forests (Hoffrén, 2024) (Lombardi, 2022), but close-range techniques are optimal if precise dendrometric attributes of the ecosystems are required. While UAV-borne LiDAR is efficient for canopy-level assessment, the pulses are mainly intercepted by the overstorey, resulting in a scarce point density at the ground and understorey levels. Regarding this point, Terrestial Laser Scanning (TLS) is a very powerful method for point cloud capturing, leading to accurate forest inventories (Moskal, 2012) or to a precise determination of forests parameters (Pitkänen, 2019). However, due to the static nature of TLS, which takes longer times for every perspective to be taken and avoid data losses, Mobile Laser Scanning (MLS) emerges as a close-range remote sensing highly viable alternative. Although the noise will be higher and the orientation of MLS will never be as accurate, these devices use Simultaneous Localization and Mapping (SLAM), which is a technology that allows them to build 3D maps of unknown environments while determining their own position at the same time. This also helps them to avoid the poor GPS signal that forests normally provide, and most of them have integrated Global Navigation Satellite System (GNSS) and Inertial Measurement Unit (IMU) components. MLS provides a significantly faster data acquisition, thanks to continuous scanning, and a reduced occlusion when an object is blocked from a single, static TLS standpoint.

In order to characterise forest parameters using MLS, several low-cost and highly accessible (Brach, 2023) devices have been developed in recent years. Studies in literature have already proved their accuracy and precision (Mitka, 2024), even in comparison to commercial systems. For instance, Balestra et al. (2024) demonstrated the high accuracy of the MandEye low-cost LiDAR device in measuring tree diameter at breast height (DBH), benchmarking it directly against two commercial handheld MLS systems (GeoSLAM ZEB HORIZON and GreenValley LiGrip H120) and a conventional TLS device, the Trimble X7.

However, while the sensor hardware determines baseline capabilities, the overarching accuracy of MLS point clouds is also dependent on the acquisition methodology. Regarding this assertion, Wang et al. (Wang, 2023) validated the structural precision of two low-cost MLS devices, with a truly complete trajectory optimisation analysis. Moreover, within complex natural forests, particularly those with dense understorey vegetation, the trajectory design directly influences the success of tree identification and structural quantification (Kuželka, 2025). In such scenarios, regular and uniform patterns of acquisition must be followed in order to avoid oversampling and noise. For example, Vandendaele et al. (2024) evaluated various mobile laser scanning cases for automated wood volume estimation in temperate forests, concluding that uniform patterns with spacing small enough to minimise occlusions are needed to achieve optimal reconstruction of forest parameters.

Given this context, and building upon these methodological premises, this project focuses on the comparison and optimisation of forest understorey data acquisition techniques using two

MLS LiDAR devices: Mandeye, a low-cost and open-source software MLS LiDAR device (Bedkowski, 2022, 2023, 2024) and FARO Orbis Premium, a commercial LiDAR handheld system, which has its own integrated software. The study was carried out in El Tello, Valencia (Spain), a Mediterranean representative pine forest. Through the standardisation of data acquisition techniques and processing pipelines, it aims to establish robust, transferable methods to derive understorey metrics from LiDAR point clouds collected using pedestrian (walking) trajectories.

2. Materials and Methods

2.1 Study site

Figure 1. Picture of the study site in El Tello, Valencia.

The study site (Figure 1) was located in the El Tello natural area, within the municipality of Llombai in the province of Valencia, Valencian Community, Spain. The dominant tree species in the canopy is Aleppo pine (*Pinus halepensis*), accompanied by a diverse understorey predominantly characterised by rosemary (*Salvia rosmarinus*) and thyme (*Thymus vulgaris*). The survey site is deliberately constrained, consisting of an approximately 10 × 10 m quadrat (see Figure 2) specifically selected to focus on understorey structural analysis.

2.2 Workflow

The general workflow and study methodology is schematised in Figure 3. Four different trajectories (see Figure 4) were followed to capture point clouds, using both devices, thus in total, eight scans were acquired. A ground control point (GCP) was taken at the spot of start and end of every scan, using a high-precision GNSS receiver. The trajectories followed were:

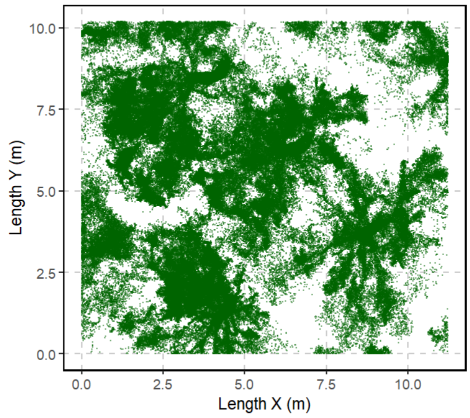

Figure 2. Top view of the dimensions (approx. 10 × 10 m) of the quadrat of study.

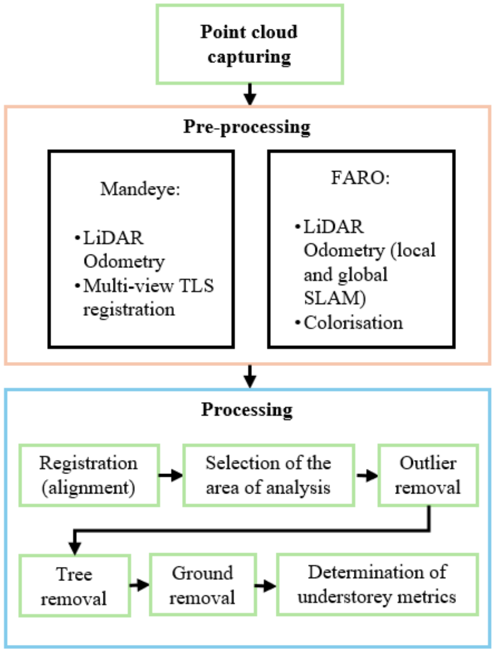

Figure 3. Study Workflow.

1. Trajectory 1 (T1): Single loop around the area of study.
2. Trajectory 2 (T2): Double loop around the area of study. Second loop is concentric to the single one, but has a greater radio.
3. Trajectory 3 (T3): Triple loop around the area of study. Second loop is concentric to the single one, but has a greater radio. Third loop is concentric to the single and double ones, but has a greater ratio.
4. Trajectory 4 (T4): 'Flower' loop around the area of study.

Once the data was acquired, a pre-processing is needed to obtain the raw point clouds (*.laz* files). Each device uses a different software system for this purpose. MandEye open-source software first performs LiDAR odometry, and then registers the views captured by the scanner. FARO's pre-processing software

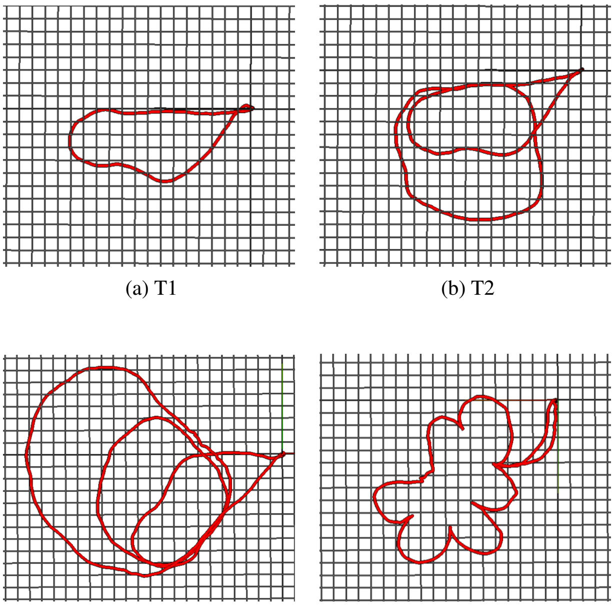

(a) T1 (b) T2

(c) T3 (d) T4

Figure 4. Trajectories top view: (a) T1 - Single loop, (b) T2 - Double loop, (c) T3 - Triple loop, and (d) T4 - ’flower’ trajectory.

(FARO Sphere XG) applies local SLAM for immediate spatial voxel-matching and global SLAM to correct accumulated drift across the entire capture. Then it colorises the geometry using integrated camera imagery and does a first outlier and noise filtering.

After this step, the raw point clouds are available for further processing. The next step consists of registering all point clouds and corresponding trajectories. This is achieved by aligning the datasets through rigid-body transformations (translations and rotations) using common points (GCP) across the different point clouds. Now that all of them are aligned, the area of study is cropped (as in Figure 1), and a statistical outlier removal filter is applied. This filter is based on calculating the average distance of each point to its nearest neighbours. Basically, if a gaussian distribution is assumed, points with an average distance higher than a specific standard deviation threshold are classified as noise and removed.

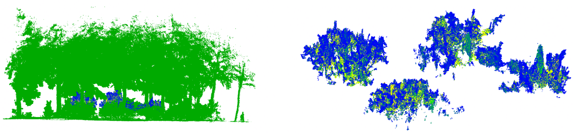

(a) (b)

Figure 5. Side view of the point clouds (T2) of the area of study, before (a) and after (b) the processing has been done. The understorey subject to analysis is colourised in blue within picture (a).

Having the point clouds prepared for manipulation, a tree removal is done using lidR (Roussel, 2020) R package, so that only the ground and understorey are kept. To isolate the ground and understorey, the point cloud undergoes height normalisation, where ground points are first classified using a Cloth Simulation Filter (CSF) algorithm (Zhang. 2016). Following normalisation, a horizontal slice of the cloud (based on the characteristics of the trees in the forest) is extracted, and a local maximum filter adapted to MLS is applied to identify the spatial locations of individual tree stems. It is to be mentioned that this is a supervised step, to make sure that no extra or non-existing stems are picked. Once they are identified, trees are removed by first applying a height threshold, and then tree stems are computationally excised by applying a 2D cylindrical exclusion buffer around the planar coordinates of each detected stem. Following the removal of tree stems and canopy elements, the dataset is further partitioned to isolate the understorey vegetation from the bare earth. This procedure successfully isolates the vegetation of interest, providing a targeted point cloud composed exclusively of the understorey structure. A supervised noise or outlier removal is again carried out, and the cloud is ready for the understorey metric (volume) extraction (see Figure 5 (b)), which is done following two methods: voxelisation (Figure 6), which depends on the resolution of voxels adjusted to the characteristics of the forests, and alpha-hull fitting (Figure 7), where alpha is the scale and detail parameter.

(a) (b)

Figure 6. Voxel fitting of the final understorey studied point clouds (T2). (b) corresponds to the zoomed-in voxelised point cloud.

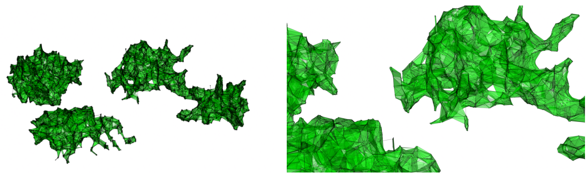

(a) (b)

Figure 7. Convex-hull (alphashape) fitting of the final understorey studied point clouds (T2). (b) corresponds to the zoomed-in hull point cloud.

Respectively, the R packages used for each model were VoxR (Lecigne, 2018) and Alphashape3d (Lafarge, 2014). Volume and mean height were chosen to be the metrics determined for this analysis because of them being relatively simple values that can well describe understorey conditions of forest ecosystems.

2.3 Description of the devices used

The two handheld LiDAR devices used for the study were MandEye and FARO Orbis Premium (Figure 8). Beginning with MandEye, it is an open-source (hardware and software) tool released by J. Bedkowski. The software characteristics are presented in (Bedkowski, 2022), a software repository consisting of an end-to-end mobile mapping framework, which is divided into three main steps (User manual v0.72 - Bedkowski, 2022):

- LiDAR Odometry: it calculates trajectory based on Lidar and IMU data.

- Multi-view TLS (Terrestrial Laser Scanner) registration.
- Multi-session registration (if needed).

On the other side, the hardware (Bedkowski, 2023) consists of Livox MID-360 sensor, a compact LiDAR designed for low speed robotics, which is based on non-repetitive scanning technology. Its effective field of view (FOV) is 360º horizontally and 59º at maximum vertically.

The theoretical point cloud density rate of the LiDAR sensor is 200000 points/s, with a minimum range (blind zone) of 0,1 m and a maximum of 40 m. Specifically, the point cloud range accuracy is stated as $\leq$ 2 cm at a distance of 10 m, and $\leq$ 3 cm at a distance of 0.2 m. Additionally, the sensor's angular accuracy is rated at $<$ 0.15º. However, detection limitations (temperature, blind zones, or other physical disturbances) must always be taken into consideration (Livox, 2024).

The sensor is supported by Raspbery Pi to manage data collection and storage, and a DJI Ronin Intelligent Battery, which works as a battery for Livox MID-360 and also as a tripod for static purposes.

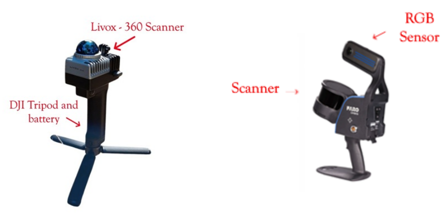

(a) (b)

Figure 8. (a) MandEye and (b) FARO Orbis Premium.

The second handheld LiDAR device used for comparison and as ground truth was FARO Orbis Premium. It is a commercial mobile mapping system which integrates LiDAR sensor with an inertial measurement unit (IMU) to perform Simultaneous Localization and Mapping (SLAM). In contrast to the architecture of MandEye, the FARO Orbis Premium operates within a closed hardware ecosystem, utilizing a proprietary datalogger and a battery for data acquisition and power management.

From the software point of view, the data collection is monitored through FARO Stream mobile application, which provides visual tracking of the trajectory during the survey. The raw *.geoslam* files generated by the device are pre-processed using FARO Sphere XG, a cloud-based platform that computes the SLAM trajectory, generates the point cloud, and applies colorisation thanks to an integrated 360º RGB camera. Regarding its hardware characteristics, the sensor provides a 360º horizontal and 290º vertical field of view (FOV), with a nominal measurement rate of 640000 points/s (FARO Technologies, 2025).

3. Results and Discussion

Table 1 summarises the point cloud densities used for the preliminary analysis, before and after manipulation, as well as the volume and mean height metrics extracted from the final point clouds.

Table 1. Point cloud density and volume estimations across the scans

	Scan	Original point cloud density[1]	Final point cloud density[2]	Volume (m^3)	Mean height (m)
VOXELISATION	T1 - MandEye	4920601	285190	4,59	0,7397
	T2 - MandEye	8256341	710494	6,82	0,7492
	T3 - MandEye	18213979	846805	7,94	0,8450
	T4 - MandEye	13299113	1275658	9,64	0,7872
	T1 - FARO	10946118	496681	7,16	0,8540
	T2 - FARO	19144825	859413	10,14	0,8590
	T3 - FARO	33727835	1257784	10,37	0,8544
	T4 - FARO	26259984	1389994	7,73	0,8693
ALPHA-HULL	T1 - MandEye	4920601	285190	6,49	0,7631
	T2 - MandEye	8256341	710494	10,07	0,8053
	T3 - MandEye	18213979	846805	11,22	0,8981
	T4 - MandEye	13299113	1275658	14,45	0,8358
	T1 - FARO	10946118	496681	11,95	0,8801
	T2 - FARO	19144825	859413	16,40	0,8931
	T3 - FARO	33727835	1257784	16,36	0,8924
	T4 - FARO	26259984	1389994	12,33	0,9102

[1] No outlier or noise filter applied.
[2] Noise filter applied. Trees and ground points removed.

The primary objective of this analysis is to evaluate the performance and robustness of a low-cost, open-source SLAM system - MandEye, in comparison with a commercial one - FARO; across different data acquisition techniques, and following a defined pipeline to determine forest metrics. This involves determining the optimal scanning trajectory for forested environments, with a specific focus on the understorey, and testing hypotheses, such as whether the execution of additional scanning loops yields a justifiable improvement in data quality.

As previously introduced, the FARO Orbis Premium capture capacity and precision is higher (see Figure 9), and so, it will be taken as ground truth throughout the analysis. It is also to be mentioned that the number of scans are reduced, but they may help to extract some conclusions which will be helpful for the complete project. Taking into account all these premises, the interpretation of the data is as follows.

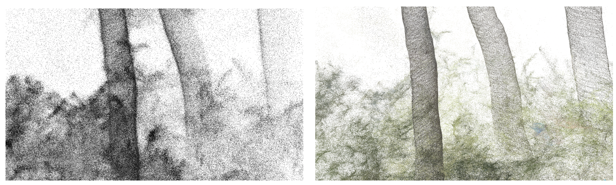

(a) (b)

Figure 9. (a) MandEye and (b) FARO raw point clouds.

Although both instruments are handheld, their hardware specifications result in disparate understorey mapping capabilities. Observing the transition from the first to the second scan (T1 to T2), the MandEye recorded a substantial proportional increase in retained points (from approximately 285k to 710k). This relative increase was notably higher than the point cloud density change observed in the FARO system for the same scans (from approximately 496k to 859k points). However, despite this high accumulation of points, the volumetric metrics (both voxelised and alphashape) generated by the MandEye remained restricted. Using FARO as ground truth, this systematic underestimation in volume is quantified by a mean negative bias of -1.60 m^3 for the voxelisation approach and -3.71 m^3 for the alpha-shape method across the datasets. Voxelisation proved to be the more reliable estimation method for the low-cost scanner in this case, but the volume bias between MandEye results and the ground truth is still very substantial, taking into account the volume sizes that are being determined. It must be acknowledged, however, that these deviations are not only induced by the devices used. The computational pipeline that has been carried out to extract these metrics (height normalisation, statistical outlier removal, algorithmic tree-stem deletion, and the geometric approximations inherent to voxelisation and alpha-shape generation) inevitably propagates and compounds spatial uncertainties.

Nonetheless, even the execution of three complete loops with the MandEye (T3) failed to reach the point cloud density and the structural volume captured by the FARO in just two loops (T2). From a technical perspective, it is proposed that this may indicate that the MandEye's laser (Livox) has lower vegetation penetration capabilities, likely exacerbated by a larger beam divergence and restricted multi-return processing. As a consequence, the emitted pulses reflect primarily off the outer vegetative layer, leading to a dense accumulation of points on the exterior canopy while failing to effectively map the internal, three-dimensional structure of the understorey.

Regarding the 'flower' (T4) acquisition trajectory, the initial hypothesis that was considered suggested that the physical inward and outward radial movements of the sensor would facilitate the capture of closer, higher precision point clouds without losing the spatial context of the surrounding vegetation, reducing the occlusion that the single loop scan may experience. However, the continuous sharp turns, frequent shifts in orientation (Vandendaele, 2024), and the absence of a clear peripheral loop closure served as a severe stress test for the SLAM algorithms of both instruments, particularly within such a highly occluded environment. As a result, the volumetric estimates generated by the MandEye for this trajectory exhibited an anomalous spike, reaching 9.64 m^3 (Voxelisation) and 14.45 m^3 (Alpha-Hull). This artificial inflation is attributed to SLAM drift and positional error, which could result in structural duplication and which have not been removed by the noise filters, thereby falsely expanding the computed volume. On the other side, the FARO system is interpreted to have withstood this complex trajectory significantly better. The understorey volume obtained from the FARO using voxelisation (7.73 m^3) was, as expected, lower than that achieved during the third concentric loop scan (10.37 m^3). This reduction makes sense geometrically: the FARO finely registered only the visible structure, and because the flower trajectory might have induced more blind spots (occlusions) in the central sector of the plot compared to systematic concentric loops, the total captured volume decreased.

Table 2. Volumetric and error metrics across the scans

	Scan	**Volume** (m^3)	**Volume diff. vs prev. scan** (m^3)	**Bias**[1] (m^3)	**Absolute error**[1] (m^3)	**Relative error** (%)
VOXELISATION	T1 - MandEye	4,59	–	2,57	2,57	36%
	T2 - MandEye	6,82	2,23	3,31	3,31	33%
	T3 - MandEye	7,94	1,11	2,43	2,43	23%
	T4 - MandEye	9,64	1,70	-1,91	1,91	25%
	T1 - FARO	7,16	–	–	–	–
	T2 - FARO	10,14	2,98	–	–	–
	T3 - FARO	10,37	0,23	–	–	–
	T4 - FARO	7,73	-2,63	–	–	–
ALPHA-HULL	T1 - MandEye	6,49	–	5,46	5,46	46%
	T2 - MandEye	10,07	3,57	6,33	6,33	39%
	T3 - MandEye	11,22	1,15	5,15	5,15	31%
	T4 - MandEye	14,45	3,23	-2,11	2,11	17%
	T1 - FARO	11,95	–	–	–	–
	T2 - FARO	16,40	4,44	–	–	–
	T3 - FARO	16,36	-0,03	–	–	–
	T4 - FARO	12,33	-4,03	–	–	–

[1] Calculated using FARO as the ground truth baseline.

Although errors are big due to the fact that only one sample is tested against ground truth for each scan, added to the small size of the study site, Table 2 ilustrares this phenomenon too, and corroborates the crucial influence of trajectory design on scanner performance. During the concentric loop trajectories (T1-T3), the MandEye systematically underestimated the understorey volume across both processing methods, evidenced by consistent positive bias values. However, as the scanning effort increased to three loops (T3), the volumetric precision improved, achieving the lowest relative error for the voxelisation approach (relative error being 23%). Conversely, the complex 'flower' trajectory (T4) induced a drastic shift from underestimation to overestimation, marked by a negative bias for both voxelisation (-1.91 m^3) and alpha-shape (-2.11 m^3). Although T4 nominally yielded the lowest relative error for the alpha-shape method (relative error being 17%), this statistical proximity to the ground truth is interpreted to be deceptive. It represents a coincidental convergence of two distinct phenomena induced by trajectory (following the same logic previously stated): the FARO system capturing less total volume due to the inherent central occlusions of the flower pattern, and the MandEye system artificially inflating its volume due to severe SLAM drift and structural duplication. Consequently, despite yielding seemingly favourable error percentages in certain metrics, erratic trajectories like T4 fundamentally compromise the geometric integrity of the point cloud and cannot be considered methodologically sound.

Moving on to the other evaluated metrics, mean height emerges as the most robust value in the dataset, as it avoids the uncertainties included while voxelising and alpha-hulling the point clouds. Regardless of the scanner used or the trajectory taken, the numerical mean height remains remarkably stable, hovering between 0,85 m and 0,89 m for the FARO Orbis system, and 0,74 m and 0,84 m for the MandEye system.

However, while this single scalar value suggests stability, the vertical point density distributions (Figure 10) reveal that the structural reconstruction process is highly dependent on the chosen trajectory. The single loop trajectory (T1) proves to be insufficient for both devices, resulting in irregular vertical profiles due to severe occlusions and a lack of diverse viewing angles. Executing additional concentric loops (T2 and T3) successfully stabilises the data, allowing the scanners to compensate for these occlusions and produce a more coherent, representative vertical distribution of the understorey. In contrast, the 'flower' trajectory (T4) breaks this stability. This fourth profile reinforces the previously mentioned conclusion about the erratic sensor movements, which induce severe SLAM drift, leading to structural duplication and an artificially broadened density profile.

4. Conclusions and Following Work

This preliminary study highlights the operational nuances of using MLS systems (both low-cost and commercial platforms) for understorey vegetation characterisation, particularly in heterogeneous Mediterranean forest environments. Based on the comparative analysis of the point cloud metrics determined with each of the devices, out of the four protocols that have been tested, the data demonstrate that regarding the efficiency of scanning trajectories, the double concentric loop (T2) represents the optimal acquisition protocol for capturing understorey vegetation for both evaluated instruments. The results also show that a the single loop scan (T1) is insufficient to overcome structural occlusion. Furthermore, while a third concentric bigger loop (T3) slighlty refines the precision of the determined

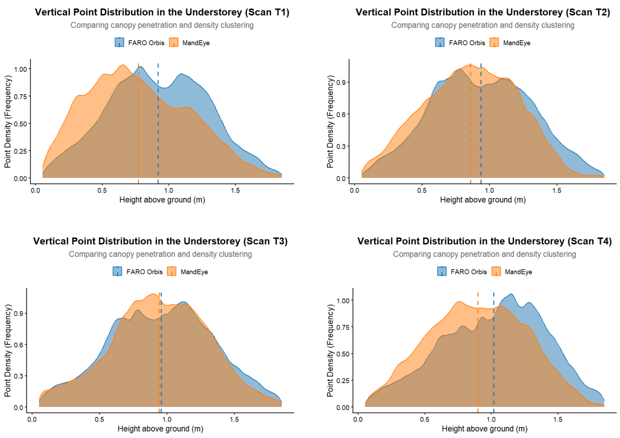

Figure 10. Vertical profile of final point cloud densities.

results and has helped to determine at what point the metric stabilisation occurs, it yields no volumetric improvements relative to the additional time and computational effort required in the field. Obviously thinking about bigger scale works to which this study is projected.

Moreover, the analysis indicates that non-uniform or complex trajectories, such as the ’flower’ pattern (T4), severely penalise SLAM algorithms. The continuous shifts in orientation might induce substantial positional drift and structural duplication, which artificially inflates point cloud density and severely compromises downstream volumetric calculations. However, despite the hardware limitations in comparison with FARO, low-cost MandEye system demonstrated significant utility. When operated within structured, predictable paths like circular loops, the open-source SLAM algorithm performs robustly. This proves that complex, erratic scanning paths are largely unnecessary and that low-cost systems can help determine highly serviceable ecological metrics when governed by disciplined field protocols.

Ultimately, the following steps of this project involve the upscaling and refinement of the work and pipelines that have been carried out. Future research will focus on scaling these findings to a broader experimental framework. The methodology will be developed across a more extensive, multi-plot study site to validate the robustness of the trajectories studies, as well as trying new ones and analysing further ecosystem metrics, across varying understorey densities and diverse forest typologies. In addition, the computational processing pipelines will be rigorously refined to minimise the spatial uncertainties inevitably induced at each methodological step. Finally, future iterations of this work will aim to incorporate algorithmic approaches designed to automatically detect and mitigate SLAM-induced structural duplication prior to volumetric calculation, thereby further enhancing the reliability of low-cost forest monitoring tools.

Acknowledgements

This research was supported by the project ‘FREs-5D: Strengthening Forest Ecosystem Resilience to Extreme Events through 5D Modelling’ (Grant number: 20253MAX003) by the Spanish National Research Council and by ‘Advancing Climate Resilience through 5D Modelling of Mediterranean Forest Ecosystems for Flood Risk Reduction (ECO-TWIN)’ (Grant number: PID2024-163036OA-I00) by the Spanish Research Agency “Knowledge Generation Projects”.

References

Balestra, M., Cabo, C., Murtiyoso, A., Vitali, A., Alvarez-Taboada, F., Cantero-Amiano, A., Bolaños, R., Laino, D. Pierdicca, R. (2024). Advancing forest inventory: a comparative study of low-cost MLS lidar device with professional laser scanners. *International Archives of the Photogrammetry, Remote Sensing and Spatial Information Sciences*, 48, 9-15.

Bedkowski, J., 2022. MapsHD/HDMapping. GitHub repository. https://github.com/MapsHD/HDMapping

Bedkowski, J., 2023. Mandeye Controller. GitHub repository. https://github.com/JanuszBedkowski/mandeye_controller

Bedkowski, J., 2024. Open source, open hardware hand-held mobile mapping system for large scale surveys. *SoftwareX, Science Direct*. 101618, https://doi.org/10.1016/j.softx.2023.101618.

Brach, M., Tracz, W., Krok, G., Gasior, J. 2023. Feasibility of Low-Cost LiDAR Scanner Implementation in Forest Sampling Techniques. *Forests*, 14(4), 706.

Casals, P., Valor, T., Besalú, A., Molina-Terrén, D. (2016). Understory fuel load and structure eight to nine years after prescribed burning in Mediterranean pine forests. *Forest Ecology and Management*. Volume 362, Pages 156-168.

Estornell, J., Ruiz, L.A., Velázquez-Martí, B., Fernández-Sarría, A. (2011). Estimation of shrub biomass by airborne LiDAR data in small forest stands. *Forest Ecology and Management*. Volume 262, Issue 9.

FARO Technologies, 2025. FARO Orbis User Manual. https://knowledge.faro.com/Hardware/Orbis/Orbis (24 March 2026).

Hoffrén, R., Lamelas, M. T., de la Riva, J. 2024. Classification and Mapping of Fuels in Mediterranean Forest Landscapes Using a UAV-LiDAR System and Integration Possibilities with Handheld Mobile Laser Scanner Systems. *Remote Sensing*, 16(18), 3536.

Kuželka, K. 2025. Trajectory design for handheld mobile laser scanning in complex natural forests: a simulation approach. *ISPRS Journal of Photogrammetry and Remote Sensing*. Volume 230.

Lafarge, T., Pateiro-López, B., Possolo, A., Dunkers, J. 2014. R Implementation of a Polyhedral Approximation to a 3D Set of Points Using the alpha-Shape. *Journal of Statistical Software*, 56(4), 1–19.

Lecigne, B., Delagrange, S., Messier, C., 2018. Exploring trees in three dimensions: VoxR, a novel voxel-based R package dedicated to analysing the complex arrangement of tree crowns, *Annals of Botany*, Volume 121, Issue 4.

Livox. (2024). Mid-360 User Manual (v1.2). Retrieved from https://www.livoxtech.com/mid-360/downloads

Lombardi, E., Rodríguez-Puerta, F., Santini, F., Chambel, M. R., Climent, J., Resco de Dios, V., Voltas, J. 2022. UAV-LiDAR and RGB Imagery Reveal Large Intraspecific Variation in Tree-Level Morphometric Traits across Different Pine Species Evaluated in Common Gardens. *Remote Sensing*, 14(22), 5904.

Mitka, B., Klapa, P., Gawronek, P. 2024. Laboratory Tests of Metrological Characteristics of a Non-Repetitive Low-Cost Mobile Handheld Laser Scanner. *Sensors*, 24(18), 6010.

Moskal, L. M., Zheng, G. 2012. Retrieving Forest Inventory Variables with Terrestrial Laser Scanning (TLS) in Urban Heterogeneous Forest. *Remote Sensing*, 4(1), 1-20.

Pitkänen, T.P., Raumonen, P., Kangas, A. 2019. Measuring stem diameters with TLS in boreal forests by complementary fitting procedure, *ISPRS Journal of Photogrammetry and Remote Sensing*, Volume 147, Pages 294-306.

Roussel, J., Auty, D., Coops, N.C., Tompalski, P., Goodbody, T.R., Meador, A.S., Bourdon, J., de Boissieu, F., Achim, A. 2020. “lidR: An R package for analysis of Airborne Laser Scanning (ALS) data.” Remote Sensing of Environment, 251, 112061. ISSN 0034-4257, doi:10.1016/j.rse.2020.112061, https://doi.org/10.1016/j.rse.2020.112061.

Vandendaele, B., Martin-Ducup, O., Fournier, R.A., Pelletier, G., 2024. Evaluation of mobile laser scanning acquisition scenarios for automated wood volume estimation in a temperate hardwood forest using quantitative structural models, *Canadian Journal of Forest Research*, Volume 54, Issue 7.

Wang, X., Yao, H., Ma, Y., Liang, X., 2023. a Comparison Study of Low-Cost Personal Laser Scanning Systems for Forest Plot-Level Inventories. *The International Archives of the Photo grammetry, Remote Sensing and Spatial Information Sciences*, 48, 1809–1815.

Zhang, W., Qi, J., Wan, P., Wang, H., Xie, D., Wang, X., Yan, G. 2016. An Easy-to-Use Airborne LiDAR Data Filtering Method Based on Cloth Simulation. *Remote Sensing*, 8(6), 501.